

The CSIW Resonator Sensor for Microfluidic Characterization Using Defected Ground Structure

Amyrul Azuan Mohd Bahar, Zahriladha Zakaria, Azmi Awang Md Isa, Yosza Dasril and Rammah A. Alahnomi
*Microwave Research Group, Centre for Telecommunication Research and Innovation (CeTRI),
Faculty of Electronic and Computer Engineering, Universiti Teknikal Malaysia Melaka (UTeM),
76100 Durian Tunggal, Melaka, Malaysia.
zahriladha@utem.edu.my*

Abstract—This paper presents a miniaturized circular substrate integrated waveguide (CSIW) resonator sensor with the integration of defected ground structure (DGS) to characterize the dielectric properties of the aqueous solvent. The sensor is developed based on the resonant perturbation method for high sensitivity and accurate measurement. The proposed structure is employed using a substrate integrated waveguide topology at 4.4 GHz with microliter (μL) volume of sample at a time. The integration of DGS structure significantly reduces the overall size of the sensor with more than 50% geometrical reduction. The changes in resonant frequency shows an identical performance based on the relative permittivity of the sample. Implications of the results and future research directions are also presented. Finally, a comparison between the proposed sensors are performed in order to identify the best sensing approach for an advancement of material characterization industry.

Index Terms—Defected Ground Structure; Microfluidic; Material characterization; Permittivity; Substrate integrated waveguide.

I. INTRODUCTION

Over the past century, there has been a dramatic increase in the development of microwave resonator sensors. The dielectric properties of materials have been studied intensively in order to improve the composition of the particular aqueous solution, especially in food and beverage industries [1], [2]. Any natural or synthetic materials has a dielectric characteristic which can be measured using resonator sensor with a different type of measuring approach such as resonant or non-resonant methods. Currently, a number of planar sensors, such as microstrip ring, coplanar waveguides, and straight ribbon have been reported to successfully detect the relative permittivity of materials with high-efficiency and accurate measurement [3]–[7]. As a result, this finding has led to many sensing application such as agriculture [8], bio sensing [9], [10], pharmaceutical [11], and chemical detection [12]–[14].

The need of well-established instruments to determine the dielectric properties of materials has gained a lot of interest. Generally, microwave sensing techniques focused on planar microwave instruments with the integration of sensitive substrate material. The latest advancement of the planar sensor for liquid characterization has been presented in [2], [15]–[18] where the dielectric response of a resonator is determined by the resonant perturbation method.

One of the latest innovation in sensor development using SIW approach is demonstrated in [17]. The microfluidic integrated microwave sensor with microliter-volume of

biological/ biomedical aqueous characterization was employed. The sensor prototype requires a minimum liquid volume of less than $7\mu\text{L}$, while still offering an overall accuracy of better than 3%, as compared with the commercial and other existing works. The proposed sensor is operating at 10 GHz with low fabrication complexity, reliable, non-invasive and contactless. However, the measurement of permittivity is only focused on real part components without considering the loss factor of the material properties. This structure is consistent with the development of SIW sensor for complex permittivity measurement as presented in [19]. The proposed sensor was designed for C band application, which works on 5.75 GHz – 5.95 GHz frequency bandwidth at high sensitivity measurement and Q-factor of 334.6. However, the relative errors detection are quite high which is 5% and 7% for real and imaginary part of the complex permittivity, respectively. It is also not suitable for measurements at lower frequency band due to its geometrical dimensions.

With the same objective, Authors in [12], [16] conducted microfluidic experiments on chemical sensor application with the presence of ethanol and DI-water. Two different type of sensors were produced with similar measurement techniques at different frequency range. Both SIW chemical sensors using reflected measurement method since they designed with a single port network application.

To be noticed, the presented literature are presenting a rectangular SIW sensor technology approach. Unlike rectangular SIW counterpart, circular structure from SIW topology exhibits strong E-field strength in term of their potential to become high-sensitive sensors considering their smaller sizes and the reliable features. This is based on the electromagnetic propagation in circular waveguide structure, especially in the presence of small amount of solvent, which may reflect some extent after detecting dielectric change towards transverse mode orientation. It is well known that many structural imperfections in the SIW topology are likely to be retained in the resulting material characterization sensing application. However, the development of microwave sensors using circular SIW technology are rarely to find these days due to the certain reasons. Nevertheless, there is one research finding in [20] which is the first study of the application using circular SIW resonators for the characterization of printed circuit board (PCB) materials. Yet, there is lack of analysis towards the reliability to ensure the full functionality of the proposed sensor. Therefore, in this work, the proposed CSIW-DGS resonator sensor shows enhancement towards sensitivity in

the presence of several common solvents. The findings were presented with sorts of structural analysis to prove the concept of the outstanding performance of compact circular SIW technology in characterization application, comparable to other reported microwave sensors.

II. WORKING PRINCIPLE

The patterns of TM and TE modes need to be strictly understood in order to choose a right transverse mode for design structure. In this work, TM modes are applied due to the existence of TM mode in circular shape waveguide with the specific electric flux pattern. Circular substrate integrated waveguide cavity is perpendicular to the imaginary hollow metallic waveguide to create a TM mode as the current line of TM mode is propagated along the waveguide structure and going through the arrays of via holes. The wave equation in circular shape coordinates is given by:

$$\left(\frac{\mathcal{G}^2}{\mathcal{G}\rho^2} + \frac{1}{\rho} \frac{\mathcal{G}}{\mathcal{G}\rho} + \frac{1}{\rho^2} \frac{\mathcal{G}^2}{\mathcal{G}\phi^2} + k_c^2 \right) e_z = 0 \quad (1)$$

E_z is the field component of transverse mode for TM mode where $E_z(\rho, \phi, z) = e_z(\rho, \phi)e^{-j\beta z}$ and $k_c^2 = k^2 - \beta^2$. Since this equation is identical to condition stated in [21]. The general solutions are the same. Thus, from the equation (2), the e_z can be found as (3).

$$h_z(\rho, \phi) = (A \sin n\phi + B \cos n\phi) J_n(k_c \rho) \quad (2)$$

$$e_z(\rho, \phi) = (A \sin n\phi + B \cos n\phi) J_n(k_c \rho) \quad (3)$$

The difference between the TE solution and the present solution is that the boundary conditions can now be applied directly to e_z of (3.12) since

$$E_z(\rho, \phi) = 0 \text{ at } \rho = a \quad (4)$$

Then, know that

$$J_n(k_c a) = 0, \text{ or } k_c = \rho_{nm}/a \quad (5)$$

where ρ_{nm} is the m th root of $J_n X$, that is, $J_n(\rho_{nm}) = 0$. Values of ρ_{nm} are given in mathematical tables; the first few values are listed in Table 1 [22] and the propagation constant of the TM_{nm} mode is

$$\beta_{nm} = \sqrt{k^2 - k_c^2} = \sqrt{k^2 - (\rho_{nm}/a)^2} \quad (6)$$

The cut-off frequency of the TE mode of a circular SIW resonator is defined as

$$f_{c_{nm}} = \frac{k_c}{2\pi\sqrt{\mu\epsilon}} = \frac{\rho_{nm}}{2\pi a\sqrt{\mu\epsilon}} \quad (7)$$

where $k_c = \frac{\rho_{nm}}{a} \quad (8)$

Therefore, the first TM mode to propagate is the TM_{01} , with $\rho_{01} = 2.405$ which is referring to table 1, and ϵ is the relative permittivity of the substrate. TM_{01} mode is implemented on this design due to high centre flux density. The understanding of the transverse mode properties is significant due to the sensor behaviour.

Table 1
The performance of planar ring resonator sensor

ρ_{nm}	m = 0	m = 1	m = 2	m = 3	m = 4
n = 1	2.4049	3.8318	5.1357	6.3802	7.5884
n = 2	5.5201	7.0156	8.4173	9.7610	11.0647
n = 3	8.6537	10.1735	11.6199	13.0152	14.3726

III. DESIGN OF THE CSIW-DGS RESONATOR

A dual port microwave planar CSIW resonator sensor with the resonant frequency of 4.4GHz is designed using HFSS simulation software. The geometrical of the design structure is calculated based on a standard equation in [21]. The radius of the circular via holes, the width of the patch, the effective dielectric constant and Q-factor can be calculated using the expression (9)-(12).

Radius of circular SIW

$$a = \frac{T_{nm} \times c}{2\pi f_r \sqrt{\epsilon_r}} \quad (9)$$

Width of the patch

$$w = \frac{c}{2f_r} \sqrt{\frac{2}{\epsilon_r + 1}} \quad (10)$$

Effective dielectric constant

$$\epsilon_{eff} = \frac{\epsilon_r + 1}{2} + \frac{\epsilon_r - 1}{2} \left[1 + \frac{12h}{w} \right]^{-1/2} \quad (11)$$

Q-factor

$$Q = \frac{2f_c}{BW} \quad (12)$$

The first design of CSIW resonator sensor working at the same frequency as CSIW-DGS which develop to characterize the dielectric properties of aqueous solvents. RT/duroid 5880 laminates glass microfiber reinforced PTFE composites are designed for exacting microstrip circuit applications. The dielectric constant of the substrate is $\epsilon_r = 2.2$ and tangent loss of $\tan \delta = 0.0009$ was employed for better electrical properties over frequency. The thickness of the substrate, h is 3.175 mm due to the necessities of the large scale of the sensing region. The substrate material is easily machined to shape the desired structure. They are resistant to all solvents and reagents, with different temperature, normally used in etching printed circuits or in plating edges and holes. Most importantly, the material has an excellent chemical resistance since the research work is dealing with liquid materials. However, the masking over the whole copper plates is compulsory to avoid oxidation and prevent any harmful towards device surface area.

Both coupling gaps at the feedlines for both designs (CSIW and CSIW-DGS) are 0.2 mm and 0.3 mm,

respectively which is the main idea to control the strength of the sensor capacitance. There are 62 plated through hole (PTH) vias with a circular shaped with grounding from the top patch to the ground as presented in previous design (CSIW with 74 vias). The coupling and feedline area, control the electromagnetic movement to constrain the wave propagating into the device. The miniaturized resonator sensor has an overall dimension of $36.16\text{mm} \times 36.16\text{mm} \times 3.245\text{mm}$ ($l_s \times w_s \times h$), after an optimization instead of the first design which having $79.92\text{mm} \times 79.92\text{mm} \times 3.245\text{mm}$ ($l_s \times w_s \times h$). The integration of defected structure contributes 50% overall size reduction over the same frequency and enhance the performance in terms of Q-factor and sensitivity. Figure 1 and Figure 2 shows both design structures with the presence of microfluidic channel.

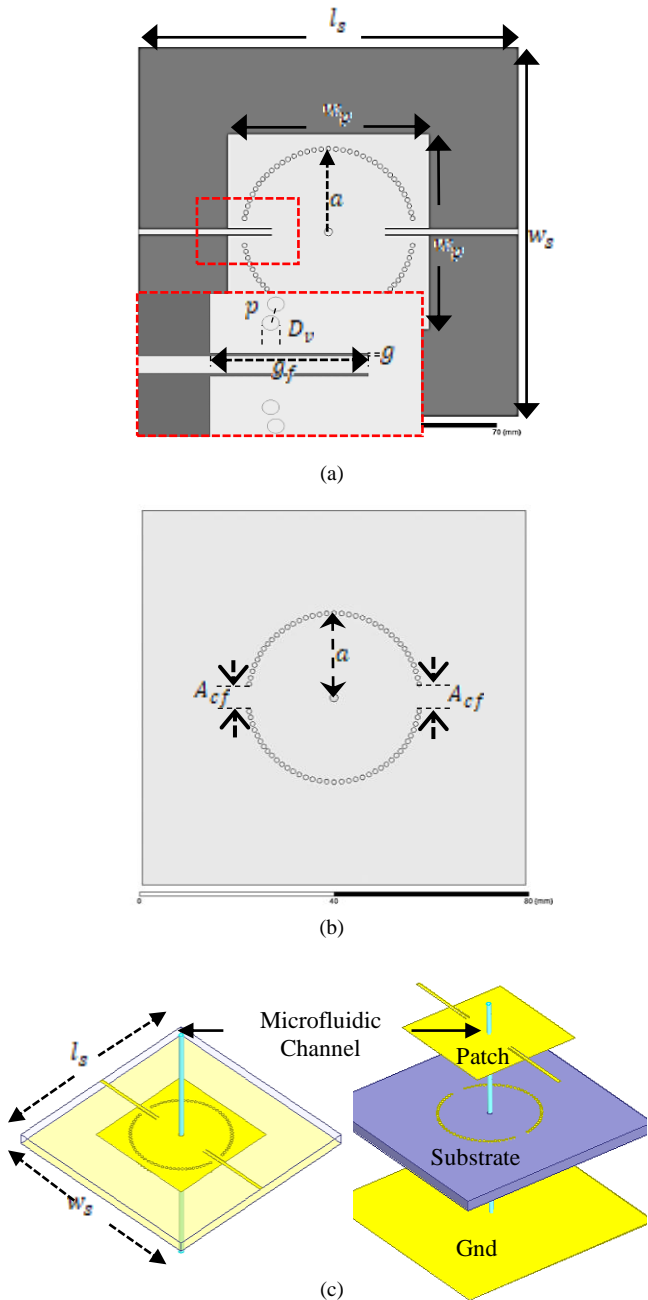


Figure 1: (CSIW) Resonator design structure. (a) Top view of the ring structure, (b) Bottom view with a layer of bare copper (c) Perspective view and layer structures integrated with microcapillary channel

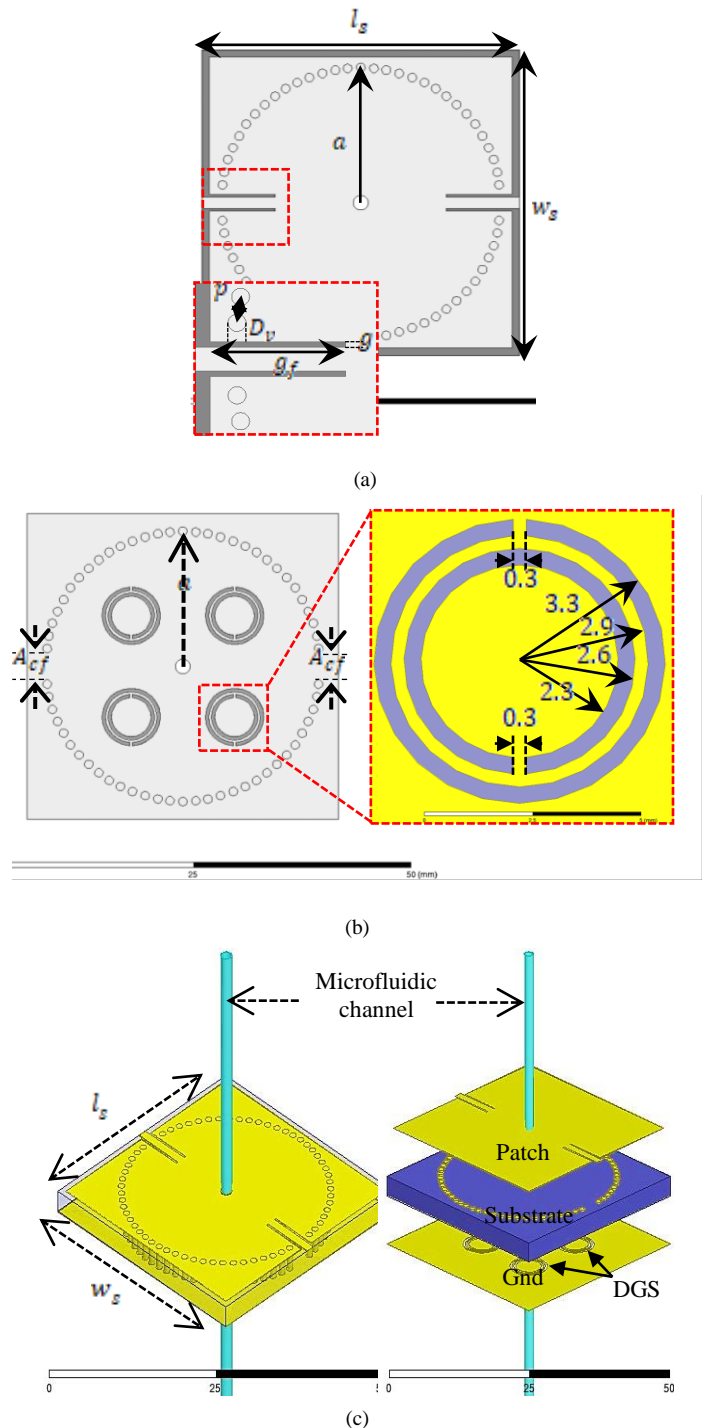


Figure 2: CSIW-DGS resonator design structure. (a) Top view of the ring structure, (b) Bottom view with DGS structure (c) Perspective view and layer structures integrated with microcapillary channel

The RT/Duroid 5880 laminate with electrodeposited copper of 1 ounces ($35\mu\text{m}$) on both sides and masking with gold conductivity to protect the copper plate layers. The introduction of DGS in the ground sensor gives an advantage of effectively reduced overall circuit size without degrading the output response. DGS structure and its position relative to the transmission line considered as practical concerns such as a size/shape that does not overlap other portions of the circuit, or a structure that can be easily trimmed to the desired center frequency. The deflection in the transmission line creates resonances, and many novels, compact microwave components and various planar circuits can be

realized by using the advantages and characteristics of DGS integration.

Simulation performed with a presence of common solvents over 1-6 GHz range frequency while corresponding resonant frequency for each liquid sample has been recorded. The glass microfluidic channel is employed with 5.5 of dielectric constant. The diameter of the glass microfluidic channel is 1 mm were located in the center device. High electric flux density was reformed with the presence of DGS structure as presented in section IV. At this point, the sensor was fabricated at very high Q-factor in order to perform with the extremely small volume of samples ($2.5 \mu L$). So that the selection dimension of the capillary was chosen at small standard size as microliter (μL) volume.

IV. RESULTS AND DISCUSSION

A. Defected Ground Structure Analysis

Material characterization demands the availability of efficient, compact, and portable devices that can be operated at high sensitivity, fast response and at low signal powers. Therefore, a depth analysis towards physical structure need to fulfill the minimum requirements in order meet the characteristics of the device. The DGS analysis structure was performed to provide better understanding towards the double split ring resonator (SRR) structure. The proposed DGS analysis consists of two axis's, x and y . Each axis involves three types of SRR structure which is double, inner and outer SRR. Best orientations position of DGS were investigated as illustrated in Figure 3 to Figure 7. The comparison between x -axis and y -axis are discussed and explained further to determine the stringent requirements of the future sensor system.

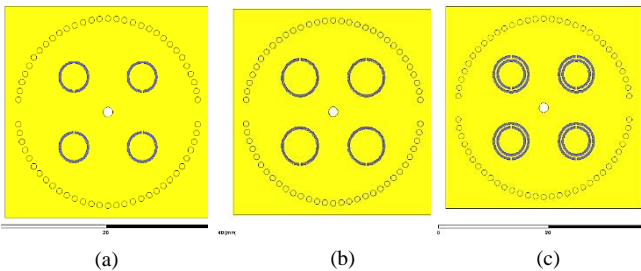


Figure 3: The y -axis of SRR structure (a) 4 symmetrical inner SRR (b) 4 symmetrical outer SRR (c) 4 symmetrical double SRR

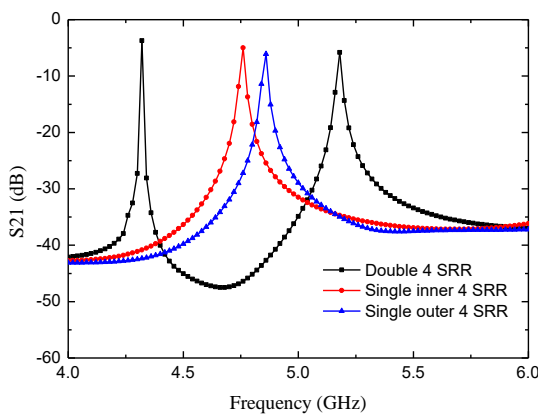


Figure 4: The frequency response of x -axis SRR structure with 4 symmetrical orientation

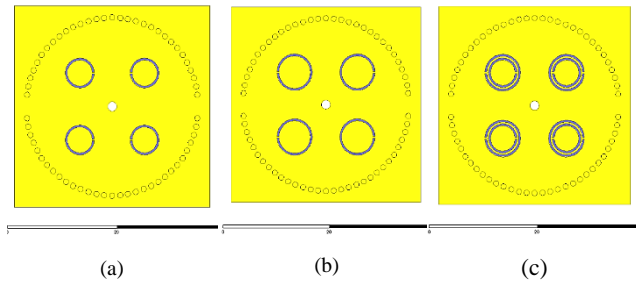


Figure 5: The y -axis of SRR structure (a) 4 symmetrical inner SRR (b) 4 symmetrical outer SRR (c) 4 symmetrical double SRR

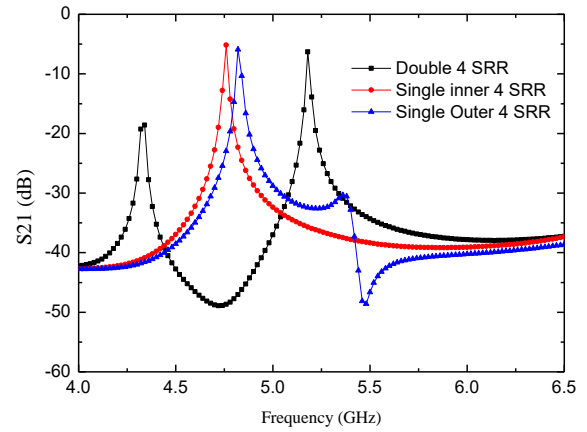


Figure 6: The frequency response of y -axis SRR structure with 4 symmetrical orientation

In Figure 4, the sensor size miniaturizing contributes to the shifting of resonant frequency towards high resonance signal. Single inner and outer DGS structure resonate at 4.76 GHz and 4.86 GHz, respectively which is still not trimmed to the desired centre frequency. However, the employment of double symmetrical DGS structure generates minimum insertion loss at 4.4 GHz due to additional harmonics.

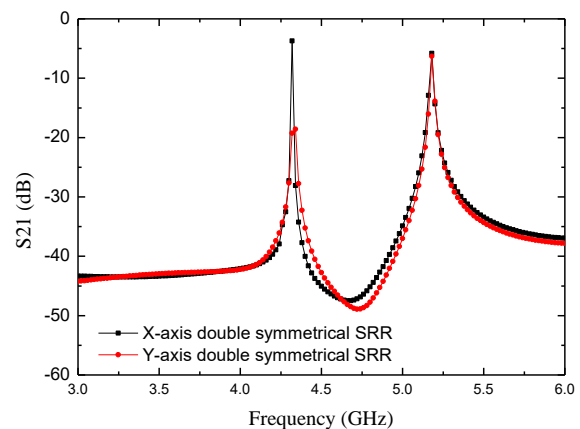


Figure 7: The comparison between 4 double symmetrical SRR for both axis

A similar response is shown in Figure 6 where the single inner and outer DGS structure resonate at high frequency instead of double SRR structure. However, the amplitude suffers from poor loss value which approximately less than 20dB. Figure 7 shows that the resonant frequency of double 4 symmetrical SRR structure for both axes. The first mode of x -axis presented an identical performance due to the S_{21} value of -3.7dB with a narrow bandwidth of 5.3MHz instead

of y -axis which required -18.6dB of S_{21} . The Q-factor of x -axis DGS structure is 1630 which far more greater than the conventional CSIW sensor. Therefore, the x -axis DGS structure were implemented in the design to enhance the performance and miniaturize an overall sensor size. The comparison of the proposed sensor between CSIW without DGS and with the presence of DGS are illustrated in Figure 8 where DGS produce resonance harmonics to reach 4.4GHz and improved the sensitivity of the sensor. On the other hand, the electric fields current propagate surround the metallic walls of the sensor. The EM wave propagation is converging on TM_{010} as the maximum E-flux were focused on the centre medium.

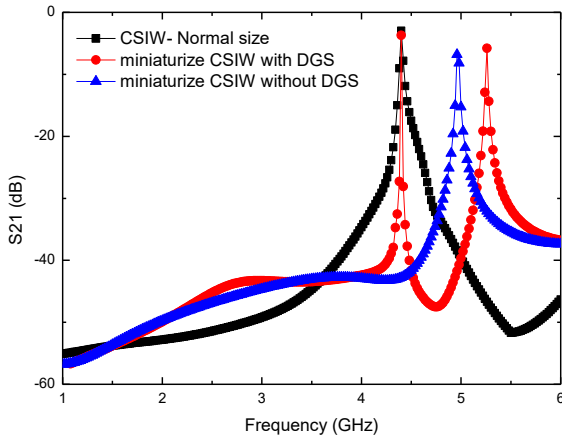


Figure 8: The frequency responses of the CSIW-DGS resonator model

B. Frequency Response with the Presence of Solvents

The proposed sensor were simulated using several aqueous solvents with the simple procedure of sample preparation. In Figure 9, the simulation response of the miniaturized CSIW-DGS sensor is demonstrated with the presence of an aqueous solvent at different relative permittivity which are; ethanol, methanol and water (24.5, 32.7, and 80.1 respectively). The first mode of the frequency response are considered as the main resonance due to the design calculation of the SRR structure. The results are identical with the perturbation theory as a high permittivity of solvents contributes to low resonant frequency and vice versa.

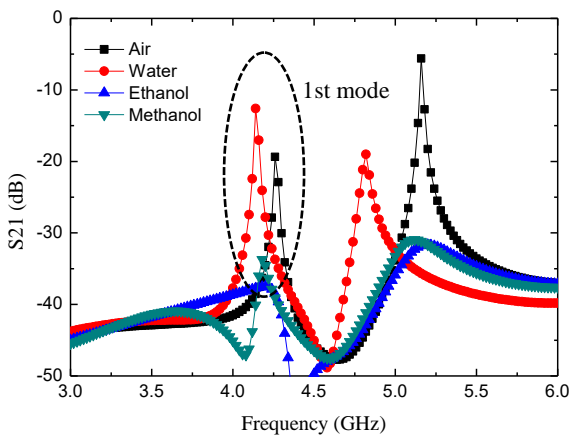


Figure 9: The frequency response of CSIW-DGS sensor with the presence of common solvents

The dataset from the first mode of the resonant frequency were extracted to develop a numerical model. From that particular derivation, the relative permittivity of the sample can be determined accurately and by using a similar method, the Q-factor of each sample can be manipulated to identify the loss tangent of each sample. However, the numerical model is valid if the dataset generates from measurement results. Further investigation and experimentation into sample concentration and volume are strongly recommended with the prototype sensor. A number of possible future studies using the same experimental set up are apparent. If the debate is to be moved forward, a better understanding of generating a mathematical model using fitting technique needs to be developed in order to investigate the dielectric properties of the liquid sample.

Table 2 shows the state-of-the-art chronology designs of several SIW resonator sensors since years 2014 until 2016. The review shows a circular design of SIW resonator sensor is rarely to find and most of the measurement are only characterized the complex permittivity and dielectric constant without considering loss tangent of material. Type of physical state of samples plays an important role in selectively suitable methods to maximize the performance of the sensor.

Table 2: The comparison of microwave SIW resonator designs from several researchers

Year	Type of resonator sensors	Geometrical structures	Measurement
2014 [23]	SIW Wireless Sensor	Rectangular	Complex permittivity
2014 [24]	SIW Cavity Based RF Sensor For	Rectangular	Complex permittivity
2015 [25]	SIW Cavity Resonator	Rectangular	Humidity Sensing
2015 [19]	SIW Resonator Sensor	Rectangular	Dielectric constant
2016 [12]	SIW Chemical Sensor	Rectangular	Frequency shifted
2016 [16]	Eighth-Mode SIW Chemical Sensor	Rectangular	Concentration
2016 [17]	Microfluidic-Integrated SIW Lab-on-Substrate Sensor	Rectangular	Dielectric constant
2016 [26]	Dielectric Perturbed Substrate Integrated Resonators	Rectangular	Hydrogen detection
2017 [This work]	CSIW-DGS planar resonator sensor	Circular	Dielectric properties

V. CONCLUSION

A microwave planar resonator sensor based on circular SIW with the integration of defected ground structure (DGS) has been designed and simulated. The proposed sensor is designed for accurate dielectric properties measurement of a microfluidic sample with $2.5\mu\text{L}$ volume at a time. The efficiency of the structure of the design with the presence of aqueous solvents is determined using HFSS simulation software. The integration of DGS structure increase the overall performance and provides high sensitivity with Q-factor more than 1600 for accurate measurement. The presence of common solvents encapsulated into the microfluidic channel is response identically as theoretical expectation. The proposed structure shows better performance in terms of the quality factor, resonant shifting, electric fields distribution, and insertion loss compared to CSIW resonator sensor without DGS.

ACKNOWLEDGMENT

Sincerely to express the appreciation to Universiti Teknikal Malaysia Melaka (UTeM) and Ministry of Higher Education (MOHE) for funding this work under the research grant FRGS/1/2015/SG02/FKEKK/03/F00265 and UTeM Zamalah Scheme.

REFERENCES

- [1] J. Tang, "Unlocking Potentials of Microwaves for Food Safety and Quality,," *Journal of food science*, vol. 80, no. 8, pp. E1776-93, 2015.
- [2] H. Samant, A. K. Jha, and M. J. Akhtar, "Design of coplanar dual band resonator sensor for microwave characterization of dispersive liquids," *IEEE MTT-S International Microwave and RF Conference, IMaRC*, pp. 249–252, 2016.
- [3] C. Watts, S. M. Hanham, M. M. Ahmad, M. Adabi, and N. Klein, "Coupled dielectric-split ring microwave resonator for liquid measurements in microfluidic channels at nanoliter volumes," *46th European Microwave Conference, EuMC 2016*, pp. 257–260, 2017.
- [4] R. Alahnomi, E. Ruslan, and S. A. Rashid, "High-Q Sensor Based on Symmetrical Split Ring Resonator with Spurlines for Solids Material Detection," *IEEE Sensors*, no. c, 2017.
- [5] A. A. M. Bahar, Z. Zakaria, S. R. A. Rashid, A. A. M. Isa, and R. A. Alahnomi, "High-Efficiency Microwave Planar Resonator Sensor Based on Bridge Split Ring Topology," *IEEE Microwave and Wireless Components Letters*, vol. 27, no. 6, pp. 545–547, 2017.
- [6] P. M. Narayanan, "Microstrip transmission line method for broadband permittivity measurement of dielectric substrates," *IEEE Transactions on Microwave Theory and Techniques*, vol. 62, no. 11, pp. 2784–2790, 2014.
- [7] A. Talai, S. Mann, R. Weigel, and A. Koelpin, "A Grounded Coplanar Waveguide Resonator Based In-Line Material Characterization Sensor," *Microwave Conference (GeMiC)*, pp. 457–460, 2016.
- [8] A. Szyplowska, A. Wilczek, M. Kafarski, and W. Skierucha, "Soil Complex Dielectric Permittivity Spectra Determination Using Electrical Signal Reflections in Probes of Various Lengths," *Vadoso Zone Journal*, vol. 15, no. 3, 2016.
- [9] Z. Wang, X. Fan, and S. Yuan, "Design and fabrication of field-effect biosensors for biochemical detection," *IET Nanobiotechnology*, vol. 8, no. 4, pp. 208–215, 2014.
- [10] S. Pinon et al., "Fabrication and characterization of a fully integrated biosensor associating microfluidic device and RF circuit," *IEEE MTT-S International Microwave Symposium Digest*, pp. 7–9, 2012.
- [11] Y. Nikawa, "Measurement of temperature dependent permittivity of liquid under microwave heating," *IEEE MTT-S International Microwave Symposium Digest*, pp. 4–7, 2016.
- [12] M. U. Memon and S. Lim, "Substrate-Integrated-Waveguide Based Chemical Sensor," *KIEES Summer Conference*, no. July, pp. 2–4, 2016.
- [13] Z. Z. Abidin, F. N. Omar, P. Yogarajah, D. R. A. Biak, and Y. B. C. Man, "Dielectric characterization of liquid containing low alcoholic content for potential halal authentication in the 0.5-50 GHz range," *American Journal of Applied Sciences*, vol. 11, no. 7, pp. 1104–1112, 2014.
- [14] G. Galindo-Romera, F. Javier Herraiz-Martínez, M. Gil, J. J. Martínez-Martínez, and D. Segovia-Vargas, "Submersible Printed Split-Ring Resonator-Based Sensor for Thin-Film Detection and Permittivity Characterization," *IEEE Sensors Journal*, vol. 16, no. 10, pp. 3587–3596, 2016.
- [15] L. Benkhaoua, M. T. Benhabiles, S. Mouissat, and M. L. Riabi, "Miniaturized Quasi-Lumped Resonator for Dielectric Characterization of Liquid Mixtures," *IEEE Sensors Journal*, vol. 16, no. 6, pp. 1603–1610, 2016.
- [16] Y. Seo, M. U. Memon, and S. Lim, "Microfluidic Eighth-Mode Substrate-Integrated-Waveguide Antenna for Compact Ethanol Chemical Sensor Application," *IEEE Transactions on Antennas and Propagation*, vol. 64, no. 7, pp. 3218–3222, 2016.
- [17] E. Silavwe, N. Somjit, and I. D. Robertson, "A Microfluidic-Integrated SIW Lab-on-Substrate Sensor for Microliter Liquid Characterization," *IEEE Sensors Journal*, vol. 16, no. 21, pp. 7628–7635, 2016.
- [18] A. A. M. Bahar, Z. Zakaria, S. R. A. Rashid, A. A. M. Isa, R. A. Alahnomi, and Y. Dasril, "Microfluidic planar resonator sensor with highly precise measurement for microwave applications," in *2017 11th European Conference on Antennas and Propagation, EUCAP 2017*, 2017.
- [19] C. Liu and F. Tong, "An SIW Resonator Sensor for Liquid Permittivity Measurements at C Band," *IEEE Microwave and Wireless Components Letters*, vol. 25, no. 11, pp. 751–753, 2015.
- [20] D. Zelenchuk and V. Fusco, "Dielectric characterisation of PCB materials using substrate integrated waveguide resonators," *European Microwave Conference (EuMC)*, no. 1, pp. 8–11, 2010.
- [21] D. Pozar, *Microwave Engineering Fourth Edition*. 2005.
- [22] L. F. Chen, C. K. Ong, C. P. Neo, V. V. Varadan, and V. K. Varadan, *Microwave Electronics*. 2004.
- [23] H. Lobato-Morales, A. Corona-Chavez, J. L. Olvera-Cervantes, R. A. Chavez-Perez, and J. L. Medina-Monroy, "Wireless sensing of complex dielectric permittivity of liquids based on the RFID," *IEEE Transactions on Microwave Theory and Techniques*, vol. 62, no. 9, pp. 2160–2167, 2014.
- [24] A. K. Jha and M. J. Akhtar, "SIW cavity based RF sensor for dielectric characterization of liquids," *IEEE Conference on Antenna Measurements and Applications, CAMA*, 2014.
- [25] H. El Matbouly, N. Boubekeur, and F. Domingue, "Passive Microwave Substrate Integrated Cavity Resonator for Humidity Sensing," *IEEE Transactions on Microwave Theory and Techniques*, vol. 63, no. 12, pp. 4150–4156, 2015.
- [26] M. Ndoye, H. El Matbouly, Y. N. Sama, D. Deslandes, and F. Domingue, "Sensitivity evaluation of dielectric perturbed substrate integrated resonators for hydrogen detection," *Sensors and Actuators, A: Physical*, vol. 251, pp. 198–206, 2016.